Journal Pre-proofs

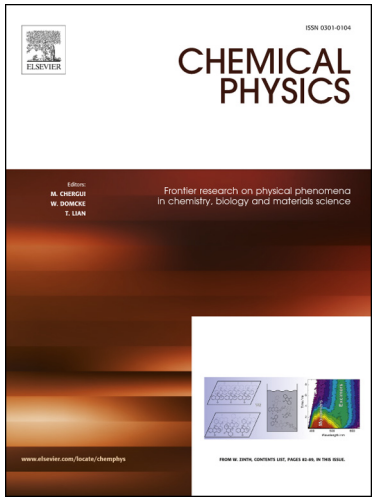

Effect of quantum corrections on thermodynamic properties for dimers

Ridha Horchani, Haikel Jelassi

PII: S0301-0104(19)31442-9
DOI: https://doi.org/10.1016/j.chemphys.2020.110692
Reference: CHEMPH 110692

To appear in: *Chemical Physics*

Received Date: 7 December 2019
Revised Date: 13 January 2020
Accepted Date: 22 January 2020

Please cite this article as: R. Horchani, H. Jelassi, Effect of quantum corrections on thermodynamic properties for dimers, *Chemical Physics* (2020), doi: https://doi.org/10.1016/j.chemphys.2020.110692

Effect of quantum corrections on thermodynamic properties for dimers

Ridha Horchani[a], Haikel Jelassi[a,b]

[a]*Department of Physics, College of Science, Sultan Qaboos University, P.O. Box 36, P. C. 123, Al-Khod, Muscat, Sultanate of Oman*
[b]*Laboratory on Energy and Matter for Nuclear Sciences Development (LR16CNSTN02), National Center for Nuclear Sciences and Technologies, Sidi Thabet Technopark 2020 Ariana, Tunisia*

Abstract

We have calculated the effect of quantum correction (QC) on the vibrational partition function by using improved Rosen-Morse potential for Cs_2 molecules. The related thermodynamics properties i.e vibrational mean energy, vibrational specific heat, vibrational free energy and vibrational entropy are derived. The change in the partition function and thermodynamic properties by adding quantum corrections up to 20^{th} order are discussed and then compared with their classical counterpart.

Keywords: Quantum correction, Partition function, Thermodynamics Proprieties, Dimers

1. Introduction

Cesium dimer has received considerable attention both theoretically and experimentally due to their large number of applications in statistical mechanics and molecular physics [1, 2]. It plays also an important role in ro-vibrational cooling of molecules and population dynamics [3, 4]. Temperature-dependant thermodynamic functions of gases over the whole temperature range from zero to the thermal dissociation limit have aroused much interest in dealing with diatomic and polyatomic systems [5, 6, 7, 8, 9, 10, 11, 12, 13, 14, 15]. Those properties are evaluated by using the vibrational partition function which is calculated in terms of molecular vibrational energy levels. Ro-vibrational energy levels and wave functions for diatomic molecules

are obtained from the direct solutions of the Schrödinger equation with diatomic molecule potential energy models [16, 17]. Many different attempts [5, 6, 18, 19, 20] have been employed to figure out approximate solutions for partition function using different techniques but each have limitations, especially at high temperature where approximation breaks down. Among them, we cite Poisson summation formula [21], commulant expansion method [22] and Wigner–Kirkwood formulation [23]. The major advantage of the classical approach is the appreciably smaller computational cost in comparison to the quantum one, which allows a treatment of molecular systems with a large number of degrees of freedom. Yet, it is well-known that classical partition function overestimates the quantum partition function at low temperatures because of importance of quantum statistics [24], while converging to the latter at the high-temperature limit due to the effect of unbound states [24, 25]. Many authors have investigated the thermodynamics properties of diatomic molecules such as sodium dimer with Rosen–Morse potential [26], lithium dimer with improved Manning–Rosen potential model [27], potassium dimer with Rosen-Morse model [28], phosphorus dimer with improved Rosen-Morse [29, 30, 31], nitrogen with modified Rosen-Morse oscillator [32] and gaseous substances (CO, CS_2, HCl, BF) with the improved Tietz oscillator [33, 34]. Motivated by those recent achievements, we will investigate quantum correction in the partition function using Poisson-summation formula followed by quantum correction in thermodynamic properties of $3^3\Sigma_g^+$ state of Cs_2 using improved Rosen-Morse potential that can well model the interaction potential curve for the $3^3\Sigma_g^+$ [35]. The effect of adding quantum correction is compared with the classical partition function and thermodynamic state functions.

2. Vibrational partition function of a diatomic molecule

The improved Rosen-Morse potential (IRM) for diatomic molecules is modeled by [36]:

$$V_{IRM}(r) = D_e(1 - \frac{e^{\alpha r_e} + 1}{e^{\alpha r} + 1})^2 \tag{1}$$

where D_e is the dissociation energy, r is the internuclear separation, r_e is the equilibrium distance, α is a dimensionless constant which controls the range of the interaction between atoms. The potential parameter α is given by the expression:

$$\alpha = \pi c\omega_e\sqrt{\frac{2\mu}{D_e}} + \frac{1}{r_e}W(\pi c\omega_e r_e\sqrt{\frac{2\mu}{D_e}}e^{-\pi c\omega_e r_e\sqrt{\frac{2\mu}{D_e}}}) \tag{2}$$

where μ is the reduced mass of the molecule, c is the speed of light, ω_e is the equilibrium harmonic vibrational frequency and W is the Lambert function, which satisfies $x = W(x)e^{W(x)}$ [37]. By solving the time independent Schrodinger equation with the improved Rosen-Morse potential it is shown that ro-vibrational energy level expression for a diatomic molecule can be represented by [38]:

$$E_{v,J} = D_e + \frac{J(J+1)\hbar^2}{2\mu r_e^2}D_0 - \frac{\hbar^2\alpha^2}{2\mu}\left[\frac{\frac{2\mu}{\hbar^2\alpha^2}D_e(e^{2\alpha r_e}-1) + \frac{j(j+1)}{\alpha^2 r_e^2}(D_1+D_2)}{2v+1-\sqrt{1+\frac{4J(J+1)}{\alpha^2 r_e^2}D_2 + \frac{8\mu}{\hbar^2\alpha^2}D_e(e^{\alpha r_e}+1)^2}}\right.$$
$$\left. - \frac{2v+1-\sqrt{1+\frac{4j(j+1)}{\alpha^2 r_e^2}D_2 + \frac{8\mu}{\hbar^2\alpha^2}D_e(e^{\alpha r_e}+1)^2}}{4}\right]^2 \tag{3}$$

where $\hbar$ denotes the reduced Planck constant, J is the rotational quantum numbers and v is the vibrational quantum number taking integer values between 0 and v_{max}. Here v_{max} denotes the most vibrational quantum number and is given by

$$v_{max} = Int\left[\sqrt{\frac{1}{4} + \frac{2\mu D_e(e^{\alpha r_e}+1)^2}{\hbar^2\alpha^2}} - \frac{1}{2}(1+\sqrt{\frac{8\mu D_e(e^{2\alpha r_e}-1)}{\hbar^2\alpha^2}})\right] \tag{4}$$

where Int stands for the integer part function.
The dimensionless coefficients D_0, D_1 and D_2 are expressed as:

$$D_0 = 1 + \frac{1}{\alpha^2 r_e^2}(3 - 3\alpha r_e + 6e^{-\alpha r_e} + 3e^{-2\alpha r_e} - 2\alpha r_e e^{-\alpha r_e} + \alpha r_e e^{-2\alpha r_e}) \tag{5}$$

$$D_1 = \frac{2}{\alpha^2 r_e^2}(-9 + 3\alpha r_e - 3e^{\alpha r_e} + 2\alpha r_e e^{\alpha r_e} - 9e^{-\alpha r_e} - 3e^{-2\alpha r_e} - \alpha r_e e^{-2\alpha r_e}) \tag{6}$$

$$D_2 = \frac{1}{\alpha^2 r_e^2}(18+12e^{\alpha r_e}+3e^{2\alpha r_e}-2\alpha r_e e^{\alpha r_e}-\alpha r_e e^{2\alpha r_e}+12e^{-\alpha r_e}+3e^{-2\alpha r_e}+2\alpha r_e e^{-\alpha r_e}+\alpha r_e e^{-2\alpha r_e}) \tag{7}$$

By substituting equations 5, 6 and 7 in equation 3 and by taking $J = 0$, the pure vibrational energy levels become:

$$E_{v,0} = D_e - \frac{\hbar^2\alpha^2}{2\mu}\left[\frac{\frac{2\mu}{\hbar^2\alpha^2}D_e(e^{2\alpha r_e}-1)}{2v+1-\sqrt{1+\frac{8\mu}{\hbar^2\alpha^2}D_e(e^{\alpha r_e}+1)^2}} - \frac{2v+1-\sqrt{1+\frac{8\mu}{\hbar^2\alpha^2}D_e(e^{\alpha r_e}+1)^2}}{4}\right]^2 \tag{8}$$

Derivation of thermodynamics data of gaseous species requires precise knowledge of the molecular vibrational partition functions. This function can be calculated by direct discreet summation over all quantified vibrational energy levels :

$$Q(\beta) = \sum_{v=0}^{v_{max}} e^{-\beta E_{v,0}} \tag{9}$$

Where $\beta = \frac{1}{k_B T}$, k_B is the Boltzmann's constant, and T is the temperature. In the following mathematical analysis, we assume that there is no chemical or physical interaction between two molecules, and we treat diatomic molecules as rigid rotors. Therefore, the effects of ro-vibrational coupling are not taken into account.

With the help of the closed form expression of equation 8 for the vibrational energy levels, we obtain the following expression of the vibrational partition function:

$$Q(\beta) = \sum_{v=0}^{v_{max}} e^{-\beta D_e - \frac{\hbar^2\alpha^2}{2\mu}\left[\frac{\frac{2\mu}{\hbar^2\alpha^2}D_e(e^{2\alpha r_e}-1)}{2v+1-\sqrt{1+\frac{8\mu}{\hbar^2\alpha^2}D_e(e^{\alpha r_e}+1)^2}} - \frac{2v+1-\sqrt{1+\frac{8\mu}{\hbar^2\alpha^2}D_e(e^{\alpha r_e}+1)^2}}{4}\right]^2} \tag{10}$$

For a finite summation with the upper bound N, the Poisson summation formula can be written as [6]

$$\sum_{n=0}^{N} f(n) = \frac{1}{2}(f(0) - f(N+1)) + \sum_{m=-\infty}^{m=+\infty}\int_0^{N+1} f(x)e^{-i2\pi mx}\,\mathrm{d}x \tag{11}$$

Under the lowest-order approximation ($m = 0$), the above summation formula becomes the following form

$$\sum_{n=0}^{N} f(n) = \frac{1}{2}(f(0) - f(N+1)) + \int_0^{N+1} f(x)\,\mathrm{d}x \tag{12}$$

With the help of expression 12, we obtain the expression for the classical partition function, $Q_0(\beta)$,from equation 10 as

$$Q_0(\beta) = \frac{1}{2}[e^{-\beta(D_e-\lambda C_1^2)} - e^{-\beta(D_e-\lambda C_2^2)}] + \int_0^{v_{max}+1} e^{-\beta(D_e-\lambda(\frac{a}{x+b}-\frac{x+b}{2})^2)}\,\mathrm{d}x \quad (13)$$

where $\lambda = \frac{\hbar^2\alpha^2}{2\mu}$, $a = \frac{\mu}{\hbar^2\alpha^2}D_e(e^{2r_e}-1)$, $b = \frac{1}{2}[1+\sqrt{1+\frac{8\mu}{\hbar^2\alpha^2}D_e(e^{\alpha r_e}+1)^2}]$, $C_1 = \frac{a}{b} - \frac{b}{2}$ and $C_2 = \frac{a}{v_{max}+1+b} - \frac{v_{max}+1+b}{2}$.
The integral in the right hand side of equation 13 is expressed in terms of the imaginary error function. After some manipulations, we obtain the following expression of the vibrational partition function for a diatomic molecule represented by the improved Rosen-Morse potential energy model:

$$\begin{aligned} Q_0(\beta) = \frac{1}{2}e^{-\beta D_e}[e^{\beta\lambda C_1^2} - e^{\beta\lambda C_2^2} + \sqrt{\frac{\pi}{\lambda}}\frac{1}{\sqrt{\beta}}(erfi[\sqrt{\beta\lambda}C_1] - erfi[\sqrt{\beta\lambda}C_2] \\ - e^{-2\beta\lambda a}erfi[\sqrt{\beta\lambda(2a+C_1)}] + e^{-2\beta\lambda a}erfi[\sqrt{\beta\lambda(2a+C_2)}])] \end{aligned} \quad (14)$$

The imaginary error function, denoted erfi, is defined as [39]

$$erfi(z) = -ierf(iz) = \frac{2}{\sqrt{\pi}}\int_0^z t^2\,\mathrm{d}t \quad (15)$$

where erf denotes the error function, which is a special function of sigmoid shape.
In deducing expression 14 from Eq. 11, we have used the lowest-order approximation which retains only the term with $m = 0$ in Eq. 10. This term is recognized as the classical partition function where all quantum corrections are omitted. The terms with $m \neq 0$ give the quantum corrections [6] and the total partition function, Q_T, is the sum of classical partition function ($m = 0$) and quantum correction (QC) in the partition function ($m \neq 0$).

$$Q_T = Q_0 + Q_{QC} \quad (16)$$

In this work, we considered quantum corrections upto 20th order.

$$\begin{aligned} Q_T &= Q_0 + \sum_{m=-20}^{m=+20}\int_0^{v_{max}+1} e^{-\beta(D_e-\lambda(\frac{a}{x+b}-\frac{x+b}{2})^2)}e^{-i2\pi mx}\,\mathrm{d}x \\ &= Q_0 + 2\sum_{m=0}^{m=20}\int_0^{v_{max}+1} e^{-\beta(D_e-\lambda(\frac{a}{x+b}-\frac{x+b}{2})^2)}cos(2\pi mx)\,\mathrm{d}x \end{aligned} \quad (17)$$

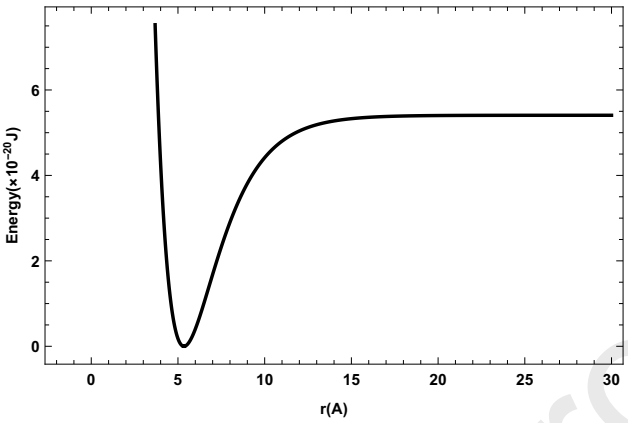

Figure 1: Potential energy function $V_{IRM}(r)$ for the $3^3\Sigma_g^+$ molecular state of Cs_2 as a function of the internuclear distance r.

In this work, we consider the Cs_2 $(3^3\Sigma_g^+)$ state as the target. For this study, experimental data of molecular constants for the chosen potential are taken from literature [38]: $D_e = 2722.28\ cm^{-1}$, $r_e = 5.3474208$ and $\omega_e = 28.8918\ cm^{-1}$. Using the above experimental values of D_e, r_e and ω_e in equation 4, we obtain the upper bound vibration quantum number as $v_{max} = 207$ for the Cs_2 $(3^3\Sigma_g^+)$ potential. Figure 1 shows the variation of V_{IRM} of equation 1 for the $3^3\Sigma_g^+$ molecular state of Cs_2 as a function of the internuclear distance r.
With the help of equation 14, we plot in Figure 2.a the classical vibrational partition function as a function of temperature for Cs_2 $(3^3\Sigma_g^+)$. The total partition functions which contains quantum correction up-to fifth-order ($m = 5$), tenth–order ($m = 10$) and twentieth–order ($m = 20$) are also shown. As expected, it is found that the partition function monotonically increases when the temperature increases. It is also shown that there is no change when adding quantum corrections at high temperature (Figure 2.a). However, figure 2.b shows that there is a significant effect in small temperature range, less then 30 K and there is no difference between high orders of quantum correction.
For a harmonic oscillator, the form of the vibrational partition function is given by [40] :

$$Q_{harm} = \frac{e^{\Theta_v/2T}}{e^{\Theta_v/T} - 1} \tag{18}$$

where $\Theta_v = \frac{hc\omega_e}{k_B}$, which is called as the vibrational characteristic temper-

ature. In figure 2.a, we report also the expression of equation 18. Figures 2.a and 2.b clearly show that the numerical values given by equation 14 are smaller than those given by equation 18 when $T < 14K$. By comparison with harmonic approximation of partition function, we infer that the classical partition function without quantum corrections is applicable when $T > 14K$. For small temperatures, results of equations 14 and 18 are similar but do not coincide with the result of equation 17. This phenomenon can be explained as that neglecting quantum effects in 14 and anharmonicity in equation 18 compensate.

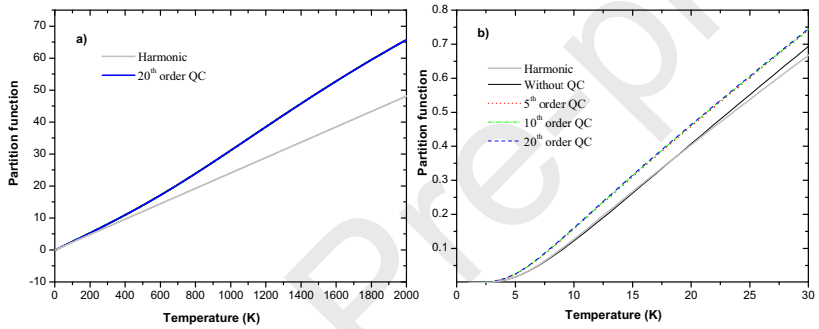

Figure 2: (a): Harmonic, classical and total (with quantum correction up-to twentieth–order ($m = 20$)) partition functions as a function of temperature for Cs_2 ($3^3\Sigma_g^+$). (b): Harmonic (Solid Gray), classical Vibrational partition function (Solid) and total partition functions with quantum correction up-to $m = 5$, 10, 20 which correspond to red dotted, green dashed-dotted and blue dashed lines, respectively, at small temperatures.

3. Thermodynamic properties

With the help of the relevant classical vibrational partition function, one can easily derive expressions of several thermodynamic proprieties such as: Vibrational mean energy U, Vibrational specific heat C, Vibrational free energy F and Vibrational entopy S.

3.1. Vibrational mean energy

The vibrational mean energy is given by

$$U_T(\beta) = -\frac{\partial ln Q_T}{\partial \beta} \tag{19}$$

where $Q_T = Q_0 + QC$ is the total partition function taking into account the quantum correction. In the case of classical partition function, U_0, is expressed as

$$\begin{aligned}
U_0(\beta) = & -\frac{\partial ln Q_0}{\partial \beta} \\
& = -\Bigg[e^{\beta\lambda C_1^2} - e^{\beta\lambda C_2^2} + \sqrt{\frac{\pi}{\lambda}}\frac{1}{\sqrt{\beta}}(erfi[\sqrt{\beta\lambda}C_1] - erfi[\sqrt{\beta\lambda}C_2] \\
& - e^{-2\beta\lambda a} erfi[\sqrt{\beta\lambda(2a+C_1)}] + e^{-2\beta\lambda a} erfi[\sqrt{\beta\lambda(2a+C_2)}])\Bigg]^{-1} \\
& \times \Bigg[-(D_e - \lambda C_1^2)e^{\beta\lambda C_1^2} + (D_e - \lambda C_2^2)e^{\beta\lambda C_2^2} - \sqrt{\frac{\pi}{\lambda}}(\frac{D_e}{\sqrt{\beta}} + \frac{1}{2\beta^{3/2}}) \\
& \times (erfi[\sqrt{\beta\lambda}C_1] - erfi[\sqrt{\beta\lambda}C_2] - e^{-2\beta\lambda a} erfi[\sqrt{\beta\lambda(2a+C_1)}] \\
& + e^{-2\beta} erfi[\sqrt{\beta\lambda(2a+C_2)}]) + \frac{C_1}{\beta}e^{\beta\lambda C_1^2} - \frac{C_2}{\beta}e^{\beta\lambda C_2^2} \\
& + \frac{2a\sqrt{\pi\lambda}e^{-2\beta\lambda a}}{\sqrt{\beta}} erfi[\sqrt{\beta\lambda(2a+C_1)}] - \frac{\sqrt{(2a+C_1)}}{\beta}e^{\beta\lambda C_1} \\
& - \frac{2a\sqrt{\pi\lambda}e^{-2\beta\lambda a}}{\sqrt{\beta}} erfi[\sqrt{\beta\lambda(2a+C_2)}] + \frac{\sqrt{(2a+C_1)}}{\beta}e^{\beta\lambda C_2}\Bigg]
\end{aligned} \tag{20}$$

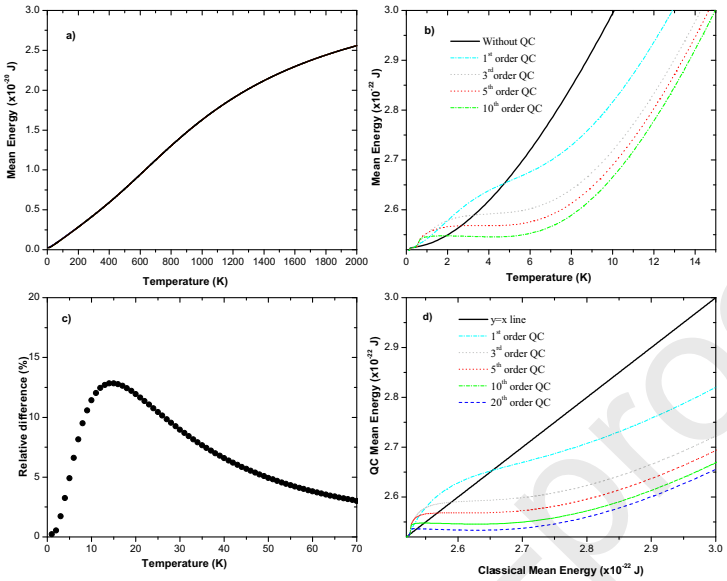

Figure 3: (a): Classical Vibrational mean energy and total mean energy with quantum correction up-to twentieth–order (m=20) as a function of temperature for Cs_2 ($3^3\Sigma_g^+$). (b): Classical Vibrational mean energy and total partition functions with quantum correction up-to m = 1,3,5, 10, 20 at small temperatures. (c): Relative difference between classical and twentieth–order quantum correction mean energies for low temperatures. (d): mean energies for different orders of quantum corrections as function of classical vibrational mean energy. To guide the eyes, $y = x$ line is also shown.

Figure 3.a displays the variation of the vibrational mean energy of cesium dimer with the temperature for both classical and with quantum correction up-to different orders. It is found that the vibrational mean energy varies monotonically with increasing the temperature. However, the figure 3.b shows that the effect of quantum corrections can be seen only for small range of temperature. At small temperature region, the increase in quantum correction terms leads to an increase in small hump.
To bring out this effect, we plot in 3.c the relative percent difference between classical vibrational mean energy and that with twentieth–order quantum correction. This resonance shape has a maximum value located at approximately $T = 15\ K$ which corresponds to the thermal energy close to the typical spacing between quantum energy levels ($k_BT = \frac{1}{2}\hbar\omega_e$) for harmonic oscillator. For more convenience, we investigate the impact of the order of quantum correction. The result is shown in 2.d where the total mean energy

with quantum correction up-to first-order ($m = 1$), third-order ($m = 3$), fifth-order ($m = 5$), tenth–order ($m = 10$) and twentieth–order ($m = 20$) are plotted as function of classical mean energy. It is clear that adding quantum correction modifies the classical mean energy ($y = x$ line).

3.2. Vibrational specific heat C

The expression of the total vibrational specific heat is given by

$$C_T(\beta) = \frac{\partial U_T}{\partial T} = -k_B\beta^2\frac{\partial U_T}{\partial \beta} \tag{21}$$

The dependence of the vibrational specific heat C with respect to temperature T is plotted in figure 4.a, which shows that the vibrational specific heat C first increases rapidly to the maximum value as the temperature increases and then decreases slowly with it. Figure 4.b shows that the increase in quantum correction from the first order to higher orders (m = 3,5,10 and 20) reveals a new maxima in the small temperature region. The position of this maxima goes to lower temperature continuously with the increase in quantum corrections. The effect of quantum corrections is most important compared to the vibrational mean energy.

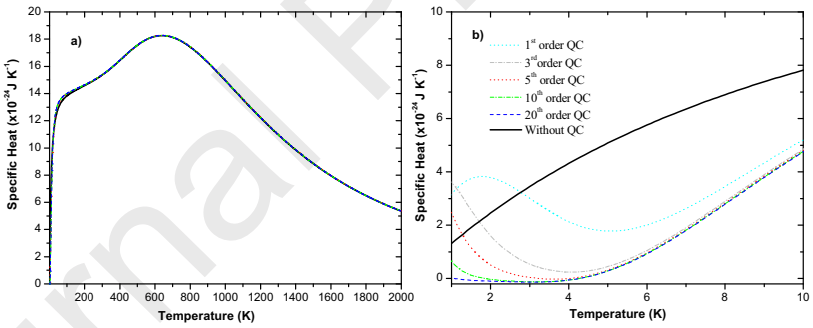

Figure 4: Vibrational specific heat C as a function of temperature T for the Cs_2 dimer. (a): Classical Vibrational specific heat C and total specific heat with quantum correction up-to twentieth–order ($m = 20$) as a function of temperature for Cs_2 ($3^3\Sigma_g^+$) potential. (b): Classical specific heat (Solid) and total specific heat C with quantum correction up-to $m = 5$, 10, 20 which corresponds to red dotted, green dashed-dotted and blue dashed lines, respectively at small temperatures.

3.3. Vibrational free energy

The expression of the total vibrational free energy is given by

$$F_T(\beta) = -k_BTlnQ_T = -\frac{1}{\beta}lnQ_T \tag{22}$$

The classical vibrational free energy is expressed by

$$F_0(\beta) = -k_B T ln Q_0 = -\frac{1}{\beta} ln Q_0$$
$$= -\frac{1}{\beta}\left[\frac{1}{2}e^{-\beta D_e}[e^{\beta\lambda C_1^2} - e^{\beta\lambda C_2^2} + \sqrt{\frac{\pi}{\lambda}}\frac{1}{\sqrt{\beta}}(erfi[\sqrt{\beta\lambda}C_1] - erfi[\sqrt{\beta\lambda}C_2]\right.$$
$$\left. - e^{-2\beta\lambda a} erfi[\sqrt{\beta\lambda(2a + C_1)}] + e^{-2\beta\lambda a} erfi[\sqrt{\beta\lambda(2a + C_2)}])\right] \quad (23)$$

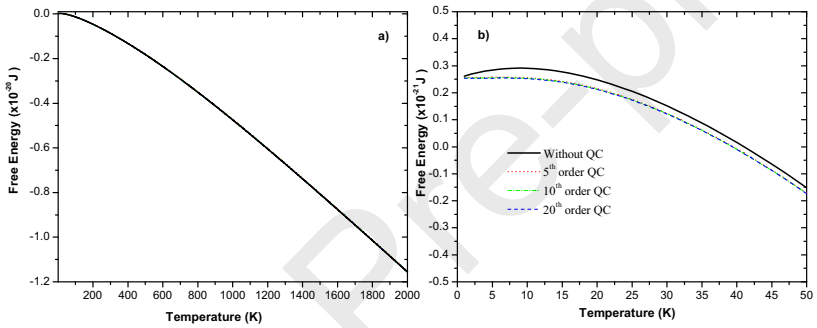

Figure 5: Classical Vibrational free energy (Solid) and total Vibrational free energy with tenth–order (m=10) quantum correction (dotted) as a function of temperature for Cs_2 ($3^3\Sigma_g^+$) up to to 2000 K (a) and for small temperatures (b).

Figure 5.a shows the calculations of the free energy according to its analytical formula given by equation 23 and 22. As it can be seen, the free energy increases to a maximum value and then it decreases monotonically with the increasing temperature. The behavior of the vibrational free energy at low temperatures is shown in Figure 5.b. Adding higher order of quantum correction decreases the maximum value of the total vibrational free energy without changing in its position located at $T = 14K$.

3.4. Vibrational entopy

The total vibrational entropy including quantum correction is given by

$$S_T(\beta) = k_B ln Q_T + k_B T \frac{\partial ln Q_T}{\partial T} \quad (24)$$

When we omit the quantum correction terms the equation 24 becomes

$$
\begin{aligned}
S_0(\beta) &= k_B lnQ + k_B T\frac{\partial lnQ}{\partial T} = k_B lnQ + k_B\beta\frac{\partial lnQ}{\partial \beta} \\
&= k_B ln\Bigg(\frac{1}{2}e^{-\beta D_e}[e^{\beta\lambda C_1^2} - e^{\beta\lambda C_2^2} + \sqrt{\frac{\pi}{\lambda}}\frac{1}{\sqrt{\beta}}(erfi[\sqrt{\beta\lambda}C_1] - erfi[\sqrt{\beta\lambda}C_2] \\
&- e^{-2\beta\lambda a}erfi[\sqrt{\beta\lambda(2a+C_1)}] + e^{-2\beta\lambda a}erfi[\sqrt{\beta\lambda(2a+C_2)}])\Bigg) \\
&- k_B\beta\Bigg[e^{\beta\lambda C_1^2} - e^{\beta\lambda C_2^2} + \sqrt{\frac{\pi}{\lambda}}\frac{1}{\sqrt{\beta}}(erfi[\sqrt{\beta\lambda}C_1] - erfi[\sqrt{\beta\lambda}C_2] \\
&- e^{-2\beta\lambda a}erfi[\sqrt{\beta\lambda(2a+C_1)}] + e^{-2\beta\lambda a}erfi[\sqrt{\beta\lambda(2a+C_2)}])\Bigg]^{-1} \\
&\times \Bigg[-(D_e - \lambda C_1^2)e^{\beta\lambda C_1^2} + (D_e - \lambda C_2^2)e^{\beta\lambda C_2^2} - \sqrt{\frac{\pi}{\lambda}}(\frac{D_e}{\sqrt{\beta}} + \frac{1}{2\beta^{3/2}}) \\
&\times (erfi[\sqrt{\beta\lambda}C_1] - erfi[\sqrt{\beta\lambda}C_2] - e^{-2\beta\lambda a}erfi[\sqrt{\beta\lambda(2a+C_1)}] \\
&+ e^{-2\beta\lambda a}erfi[\sqrt{\beta\lambda(2a+C_2)}]) + \frac{C_1}{\beta}e^{\beta\lambda C_1^2} - \frac{C_2}{\beta}e^{\beta\lambda C_2^2} \\
&+ \frac{2a\sqrt{\pi\lambda}e^{-2\beta\lambda a}}{\sqrt{\beta}}erfi[\sqrt{\beta\lambda(2a+C_1)}] - \frac{\sqrt{(2a+C_1)}}{\beta}e^{\beta\lambda C_1} \\
&- \frac{2a\sqrt{\pi\lambda}e^{-2\beta\lambda a}}{\sqrt{\beta}}erfi[\sqrt{\beta\lambda(2a+C_2)}] + \frac{\sqrt{(2a+C_1)}}{\beta}e^{\beta\lambda C_2}\Bigg]
\end{aligned}
\tag{25}
$$

Figure 6.a shows the calculation of the entropy according to its analytical formula given by equation 24 and 25. It shows that the vibrational entropy increases monotonically with temperature and then tends to reach a constant value at higher temperatures. The variation of vibrational entropy at low temperatures is shown in Figure 6.b. Adding higher order of quantum correction causes an increase in new band in the low temperature regime (less than $T = 12K$) which is similar to specific heat. However, increasing slightly the temperature leads to an inverse behaviour i.e the vibrational entropy with quantum correction becomes slightly smaller than that without quantum correction.

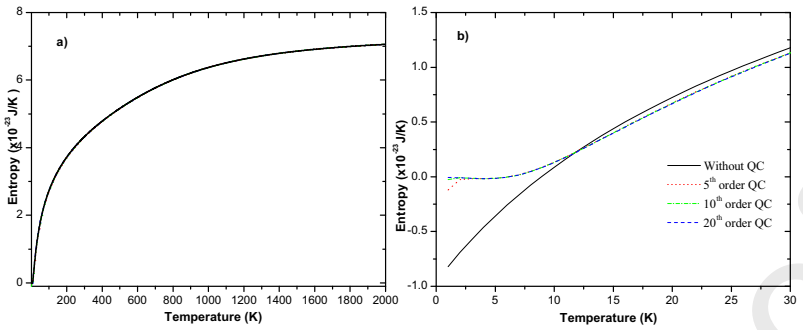

Figure 6: Vibrational entropy S as a function of temperature T for Cs_2 dimer. (a): Classical vibrational entropy S and total vibrational entropy with quantum correction up-to twentieth–order ($m = 20$) as a function of temperature for Cs_2 ($3^3\Sigma_g^+$) potential. (b): Classical vibrational entropy (Solid) and total vibrational entropy with quantum correction up-to $m = 5$, 10, 20 which corresponds to red dotted, green dashed-dotted and blue dashed lines, respectively at small temperatures.

4. Conclusion

The term quantum correction in partition function first introduced by Strekalov [5] but till now there is not any theoretical investigation present. Quantum correction upto 20th order was calculated for Cs_2 ($3^3\Sigma_g^+$) potential. The effect of quantum correction on partition function is least. The vibrational specific heat C is more sensitive to quantum correction as compared to vibrational free energy F and entropy S due to the second derivative of the partition function in C instead of first derivative in F and S. The effect of quantum correction is important in the small temperature range. The classical partition function converges to total partition function in the high temperature region and this is similar with other thermodynamic properties also.

[1] K M Kuhler, D G Truhler and A D Issacson, J. Chem. Phys. 104, 4664 (1996)

[2] A D Issacson, J. Chem. Phys. 108, 9978 (1998)

[3] I. Manai, R. Horchani, H. Lignier, P. Pillet, D. Comparat, A. Fioretti, and M. Allegrini. Phys. Rev. Lett. 109,(2012) 183001

[4] R. Horchani, H. Lignier, N. Bouloufa-Maafa, A. P. P. Fioretti, D. Comparat, Phys. Rev. A 85 (2012) 030502.

[5] M.L. Strekalov, Chem. Phys. Lett. 393 (2004) 192.

[6] M.L. Strekalov, Chem. Phys. Lett. 439 (2007) 209.

[7] Y. Babou, Ph. Rivière, M.-Y. Perrin, A. Soufiani, Int. J. Thermophys. 30 (2009) 416.

[8] Karl K. Irikura, J. Chem. Thermodyn. 73 (2014) 183.

[9] M. Buchowiecki, Chem. Phys. Lett. 635 (2015) 196.

[10] M. Buchowiecki, Chem. Phys. Lett. 652 (2016) 32.

[11] M. Buchowiecki, Chem. Phys. Lett. , Volume 687, (2017), Pages 227-232

[12] L. Sellaoui, H. Guedidi, S. Knani, L. Reinert, L. Duclaux, A.B. Lamine, Fluid Phase Equilib. 387 (2015) 103.

[13] D. Skouteris, D. Calderini, V. Barone, J. Chem. Theory Comput. 12 (2016) 1011.

[14] T.F. da Cunha, D. Calderini, D. Skouteris, J. Phys. Chem. A 120 (2016) 5282.

[15] S.I. Sandler, J. Supercrit. Fluid. 55 (2010) 496.

[16] J.Y. Liu, G.D. Zhang, C.S. Jia, Phys. Lett. A 377 (2013) 1444.

[17] X.T. Hu, L.H. Zhang, C.S. Jia, J. Mol. Spectrosc. 297 (2014) 21

[18] D. Popov, Phys. Lett. A 316 (2003) 369.

[19] F. M. Fernandez, E. A. Castro, Chem. Phys. Lett. 94 (1982) 388.

[20] I. I. Cotaescu, N. Pop, Int. J. Theor. Phys. 48 (2009) 1596.

[21] P M Morse and H Feshbash, Methods of theoretical physics (McGraw-Hill, New York, 1953)

[22] G Herzberg, Molecular spectra and molecular structure II, Infared and Raman spectra of polyatomic molecules (Van Nostrand, New York, 1945)

[23] H J Korsch, J. Phys. A: Math. Gen. 12, 1521 (1979)

[24] McQuarrie, D. A. Statistical Mechanics; Harper and Row: New York, 1976.

[25] Frederick H. Mies and Paul S. Julienne, J. Chem. Phys. 77, 6162 (1982)

[26] X Q Song, C W Wang and C S Jia, Chem. Phys. Lett. 673, 50 (2017)

[27] C S Jia, L H Zhang and C W Wang, Chem. Phys. Lett. 667, 211 (2017)

[28] C S Jia, C W Wang, L H Zhang, X L Peng, R Zeng and X T You, Chem. Phys. Lett. 676, 150 (2017)

[29] Chun-Sheng Jia, Chao-Wen Wang, Lie-Hui Zhang, Xiao-Long Peng, Hong-Ming Tang, Ran Zeng, Chemical Engineering Science, Vol, 183, Page: 26-29 (2018)

[30] Xiao-Long Peng; Rui Jiang; Chun-Sheng Jia; Lie-Hui Zhang; Yu-Long Zhao, Chemical Engineering Science, ISSN: 0009-2509, Vol: 190, Page: 122-125 (2018).

[31] Chun-Sheng Jia; Ran Zeng; Xiao-Long Peng; Lie-Hui Zhang; Yu-Long Zhao, Chemical Engineering Science, ISSN: 0009-2509, Vol: 190, Page: 1-4 (2018)

[32] Chun-Sheng Jia; Lie-Hui Zhang; Xiao-Long Peng; Jian-Xin Luo; Yu-Long Zhao; Jian-Yi Liu; Jing-Jing Guo; Lian-Dong Tang, Chemical Engineering Science, ISSN: 0009-2509, Vol: 202, Page: 70-74(2019).

[33] Xiao-Yu Chen, Ji Li,and Chun-Sheng Jia, ACS Omega (2019), 4, 14, 16121-16124

[34] Rui Jiang; Chun-Sheng Jia; Yong-Qing Wang; Xiao-Long Peng; Lie-Hui Zhang, Chemical Physics Letters, ISSN: 0009-2614, Vol: 715, Page: 186-189 (2019).

[35] X.T. Hu, J.Y. Liu, C.S. Jia, Comput. Theor. Chem., 1019 (2013), p. 137

[36] C.S. Jia, Y.F. Diao, X.J. Liu, P.Q. Wang, J.Y. Liu, G.D. Zhang, J. Chem. Phys., 137 (2012), p. 014101

[37] R.M. Corless, G.H. Gonnet, D.E.G. Hare, D.J. Jeffrey, D.E. Knuth, Adv. Comput. Math., 5 (1996), pp. 329-359

[38] J.Y. Liu, X.T. Hu, C.S. Jia, Can. J. Chem., 92 (2014), pp. 40-44

[39] C.E. Pearson, Handbook of Applied Mathematics, Van Nostrand Reinhold, New York (1983).

[40] F. Schwabl, Statistical Mechanics (second ed.), Springer-Verlag, Berlin Heidelberg (2006).